

Synthesis, structure, and electrochemistry and magnetic properties of a novel 1D homochiral Mn^{III}(5-Brsalen) coordination polymer with left-handed helical character

Dapeng Dong, Naisen Yu, Haiyan Zhao, Dedi Liu, Jia Liu, Zhenghua Li, Dongping Liu*

Liaoning Key Laboratory of Optoelectronic Films and Materials, School of Physics and Materials Engineering, Dalian Nationalities University, Dalian, PR China

ARTICLE INFO

Article history:

Received 3 July 2015

Received in revised form

9 September 2015

Accepted 29 September 2015

Available online 3 October 2015

Keywords:

Spontaneous resolution

Chirality

Crystal structure

Electrochemistry

ABSTRACT

A novel homochiral manganese (III) Mn(5-Brsalen) coordination polymer with left-handed helical character by spontaneous resolution on crystallization by using Mn(5-Brsalen) and 4,4-bipyridine, [Mn^{III}(5-Brsalen)(4,4-bipy)]·ClO₄·CH₃OH (**1**) (4,4-bipy = 4,4-bipyridine) has been synthesized and structurally characterized by X-ray single-crystal diffraction, elemental analysis and infrared spectroscopy. In compound **1**, each manganese(III) anion is six-coordinate octahedral being bonded to four atoms of 5-Brsalen ligand in an equatorial plane and two nitrogen atoms from a 4,4-bipyridine ligand in axial positions. The structure of compound **1** can be described a supramolecular 2D-like structure which was formed by the intermolecular π-stacking interactions between the neighboring chains of the aromatic rings of 4,4-bipyridine and 5-Brsalen molecules. UV-vis absorption spectrum, electrochemistry and magnetic properties of the compound **1** have also been studied.

© 2015 Elsevier B.V. All rights reserved.

1. Introduction

Chirality is an essential element for life, which plays a key role in biological system and pharmacy, as well as in advanced materials such as asymmetric catalysis, chiral separation and nonlinear optical devices [1–5]. The general approach to a chiral framework is using a chiral molecule as the primary linker or as an inducer of final chirality, which is the most effective method for the synthesis of chiral coordination polymers [6–9]. However, due to the limitation of the chiral pool and very often the high cost of chiral ligands, it is highly desirable to create chiral compounds from achiral precursors. Spontaneous resolution on crystallization without any chiral auxiliary usually yields chiral conglomerate, which has been proved as a constructive approach for the synthesis of individual chiral metal–organic coordination polymers [10–12]. However, the controllable generation of such chiral frameworks from totally achiral precursors is still of a great challenge since it may be significantly governed by several factors such as the flexibility of organic ligand, coordination geometry of the metal center, counterion, solvent, reaction temperature, and pH value of the

solution [13–19]. Moreover, spontaneous resolution is relatively rare and cannot be predicted because its mechanism is not yet fully understood.

On the other hand, tetradeятate H₂salen and salen derivatives are versatile ligands, which consisting of two nitrogen and two oxygen donors to form stable metal complexes, are very popular O- and N-donor linkers because of their excellent chelating capabilities. Salen-type N₂O₂ ligands coordinate to various kinds of transition-metal ions in a tetradeятate fashion to produce stable complexes which have found versatile applications in a wide range of areas such as catalysis, biochemistry, electrochemistry, magnetic properties, and luminescent materials [20–26]. Among them, some manganese (III) complexes of salen type Schiff base ligands have been synthesized in the past decades [27–29]. However, to the best of our knowledge, the homochiral manganese (III) Mn(5-Brsalen) coordination polymer with left-handed helical character by spontaneous resolution on crystallization have not been reported so far. In this paper, we chose an achiral 5-BrsalenMn molecule as the building unit and successfully synthesized a homochiral Mn(5-Brsalen) coordination polymer with left-handed helical character, [Mn^{III}(5-Brsalen)(4,4-bipy)]·ClO₄·CH₃OH (**1**). The crystal structure, electrochemistry and magnetic properties of compound **1** have also been studied.

* Corresponding author.

E-mail address: dongping.liu@dlnu.edu.cn (D. Liu).

2. Experimental section

2.1. General procedures

The reagents were obtained from commercial sources and used without further purification. Elemental analyses were performed on an Elementar Vario ELIII analyzer. IR spectra were recorded using KBr pellets on a Vector 22 Bruker spectrophotometer in the 4000–400 cm⁻¹ regions. The UV–Vis diffuse reflectance spectra were recorded with a JASCO V-570 UV–Vis–NIR spectrophotometer in the 300–800 nm. Cyclic voltammetry (CV) measurements were carried out on a BAS 100 W system in a three-electrode cell with a pure N₂ gas inlet and outlet. Temperature-dependent magnetic measurements were carried out on a Quantum Design SQUID MPMS-5 magnetometer with an applied field of 1 kOe, and diamagnetic corrections were made with Pascal's constants.

2.2. Synthesis of the Schiff-base ligand *N,N*-bis(5-Bromosalicylidene)ethane-1,2-diamine (5-Brsalen)

The tetradentate Schiff base ligand was prepared by the condensation of 5-Bromosalicylaldehyde (2.01 g, 10 mmol) and 1,2-ethanediamine (0.30 g, 5 mmol) in methanol (10 mL) as reported earlier [30].

2.3. Synthesis of [Mn^{III}(5-Brsalen)(H₂O)]ClO₄ (5-BrsalenMn)

The manganese(III) complex was obtained by mixing manganese(III) acetate dihydrate (5.0 mmol, 1.34 g) and 5-Brsalen (5.0 mmol, 2.13 g) in methanol (200 mL) and anhydrous sodium perchlorate (7.5 mmol, 0.92 g) in water (80 mL). After evaporation to 40 mL and cooling, the resulting black crystals were collected by suction filtration [31]. Anal. Calcd for C₁₆H₁₄N₂O₇Br₂ClMn: C, 32.22; H, 2.73; N, 4.70%. Found: C, 32.17; H, 2.70; N, 4.75%.

2.4. Synthesis of [Mn^{III}(5-Brsalen)(4,4-bipy)]·ClO₄·CH₃OH (**1**)

A solution of [Mn^{III}(5-Brsalen)H₂O]ClO₄ (0.1 mmol, 0.060 g) and 4,4-bipyridine (0.1 mmol, 0.016 g) in CH₃OH solution (20 mL) was stirred for 2 h at room temperature, and then filtered, and the filtrate was left at room temperature in the dark room for evaporation. After one week, the dark-brown crystals was collected by suction filtration, washed with water, and air-dried. Yield: 43%. Elemental analysis for compound **1**: Calc (found) for C₂₇H₂₄Br₂ClMnN₄O₇: %C 42.30 (42.36), %N 7.31 (7.35), %H 3.16 (3.18). IR (solid KBr pellet ν/cm^{-1}): 3441 br, 3082 w, 3048 w, 2965 w, 2826 w, 2854 w, 2802 w, 1624 s, 1532 w, 1451 s, 1407 m, 1371 m, 1277 m, 1179 w, 1092 s, 1005 w, 975 w, 832 w, 807 w, 690 w, 621 w, 479 w, 463 w.

2.5. X-ray crystallography

The data were collected at a temperature of 293 ± 2 K on a Bruker Smart APEX II X–diffractometer equipped with graphite monochromated Mo–K α radiation ($\lambda = 0.71073 \text{ \AA}$) using the SMART and SAINT programs. Indexing and unit cell refinement were based on all observed reflections from those 72 frames. The structure was solved in the space group P4₃2₁2 by direct method and refined by the full–matrix least–squares fitting on F^2 using SHELXTL–97 [32]. All non–hydrogen atoms were refined anisotropically and the hydrogen atoms isotropically in theoretical positions. The final cycle of full-matrix least-squares refinement was based on number of observed reflections ($I > 2\sigma(I)$). The crystal data and structure refinement of compound **1** is summarized in Table 1. Selected bond lengths (Å) and bond angles (°) for **1** is listed in

Table 1
Crystallographic data and structure refinement for compound **1**.

Formula	C ₂₇ H ₂₄ Br ₂ ClMnN ₄ O ₇
Fw	766.71
Crystal system	Tetragonal
Space group	P4 ₃ 2 ₁ 2
a, Å	16.5697(5)
c, Å	21.9035(15)
V, Å ³	6013.7(5)
Z	8
D _c , g/cm ³	1.694
μ (Mo K α), mm ⁻¹	3.237
Crystal size, mm ³	0.40 × 0.10 × 0.08
θ_{\min} , θ_{\max} , °	1.54, 27.50
No. total reflns.	26816
No. uniq. reflns (R _{int})	6847 (0.0653)
No. obs. [$I \geq 2\sigma(I)$]	4304
No. params	379
Completeness to theta = 27.50, %	99.2
R1, wR2 [$I \geq 2\sigma(I)$]	0.0817, 0.2047
R1, wR2 (all data)	0.1308, 0.2395
Absolute structure parameter	-0.02(2)
GOF	1.015

$$R_1 = \sum (|F_0| - |F_C|)/\sum |F_0|; wR_2 = [\sum w (|F_0| - |F_C|)^2/\sum w F_0^2]^{1/2}.$$

Table 2. CCDC 1026479 contains the supplementary crystallographic data for this paper. These data can be obtained free of charge via <http://www.ccdc.cam.ac.uk/conts/retrieving.html> (or from the Cambridge Crystallographic Data Centre, 12, Union Road, Cambridge CB21EZ, UK; Email: deposit@ccdc.cam.ac.uk).

3. Results and discussion

3.1. Crystal structures

Single-crystal X-ray diffraction analysis revealed that compound **1** crystallizes in the tetragonal chiral space group P4₃2₁2. The crystal structure comprised one [Mn^{III}(5-Brsalen)(4,4-bipy)]⁺ cation, one uncoordinated methanol molecule and one perchlorate anion. As shown in Fig. 1, each manganese (III) anion is six-coordinate octahedral being bonded to four atoms of 5-Brsalen ligand in an equatorial plane and two nitrogen atoms from a 4,4-bipyridine ligand in axial positions. Each 4,4-bipyridine molecule links the Mn^{III}(5-Brsalen) moieties result in the one-dimensional polymeric structure. The bond lengths in the equatorial plane fall in the range of 1.889(5)–1.895(6) Å for Mn–O, 1.978(6)–1.978(7) Å for Mn–N, while axial Mn–N distances are in the range of 2.346(6)–2.362(6) Å. Selected bond lengths and angles are summarized in Table 2. The axial bonds are significantly longer than the equatorial bonds, as expected for the Jahn–Teller distortion of Mn ions with a +3 oxidation state. The intrachain Mn···Mn distance is

Table 2
Selected bond lengths (Å) and angles (°) for complex **1**.

Mn(1)-O(1)	1.889(5)	Mn(1)-N(2)	1.978(6)
Mn(1)-O(2)	1.895(6)	Mn(1)-N(3)	2.346(6)
Mn(1)-N(1)	1.978(7)	Mn(1)-N(4)#1	2.362(6)
Br(1)-C(4)	1.907(10)	Br(2)-C(13)	1.910(9)
O(1)-Mn(1)-O(2)	97.8(2)	N(2)-Mn(1)-N(3)	95.0(2)
O(1)-Mn(1)-N(2)	172.2(3)	N(1)-Mn(1)-N(3)	91.6(3)
O(2)-Mn(1)-N(2)	89.4(3)	O(1)-Mn(1)-N(4)#1	86.6(2)
O(1)-Mn(1)-N(1)	91.0(2)	O(2)-Mn(1)-N(4)#1	88.6(2)
O(2)-Mn(1)-N(1)	171.2(3)	N(2)-Mn(1)-N(4)#1	90.7(2)
N(2)-Mn(1)-N(1)	81.8(3)	N(1)-Mn(1)-N(4)#1	91.7(3)
O(1)-Mn(1)-N(3)	88.0(2)	N(3)-Mn(1)-N(4)#1	173.7(2)
O(2)-Mn(1)-N(3)	88.9(2)		

Symmetry transformations used to generate equivalent atoms: #1 y + 1, x, -z.

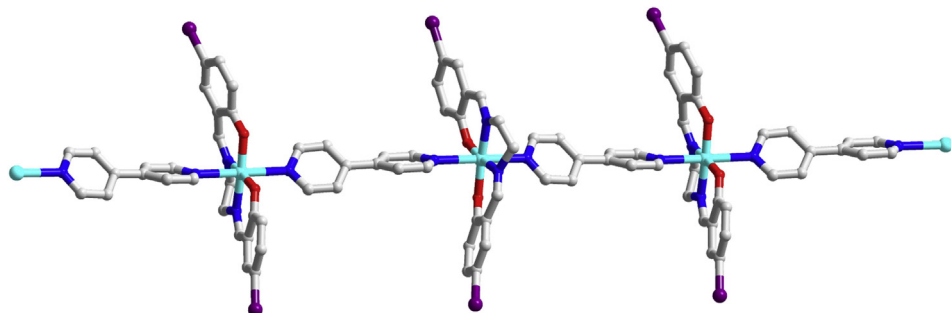


Fig. 1. Side view of a 1-D chain along the *a*-axis. All the H atoms, perchlorate anions and methanol molecules are omitted for clarity. Atomic scheme: Mn(III), turquoise; C, light gray; N, blue; Br, violet; O, red. (For interpretation of the references to color in this figure legend, the reader is referred to the web version of this article.)

11.768 Å.

In the compound, there is considerable π -stacking interactions with the centroid distance of 3.995 and 3.770 Å between the neighboring chains of the aromatic rings of 4,4-bipyridine and 5-Brsalen molecules (Fig. 2). On the basis of these connection modes, the mutual parallel 1D chains of each layer are interwoven perpendicularly to generate a two-dimensional supramolecular network (Fig. 3a), which form the left-handed helical character running along a crystallographic 4_3 axis in the *c* direction (Fig. 3b, c). Notably, the compound **1** has the same handedness and the refined value of the Flack parameter ($-0.01(2)$) shows that each crystal of the chiral framework phase grows as one single enantiomer, with a homochiral character for the helix winding. In general, two key factors are necessary to generate a homochiral coordination polymer from an achiral ligand without any chiral auxiliary [33,34]. This means that not only the achiral components must assemble into chiral units, but also these chiral units homochirally aggregate. So it is difficult to construct the homochiral helix from achiral components.

3.2. Infrared spectroscopy

The IR spectrum of compound **1** was recorded in the region from

4000 to 400 cm^{-1} , as shown in Fig. 4. The absorption bands around 3441 cm^{-1} corresponds to the vibrations of O–H stretching of methanol molecule. The bands at the region of 3082–2800 cm^{-1} are assigned to the aromatic and aliphatic C–H stretching vibrations, and the strong bands at the region of 1532–1371 cm^{-1} are assigned to the aromatic C=C stretching vibrations. The sharp peaks at 1624 related to the C=N groups in compound **1**, while the strong band at 1451 attributed to the aromatic C=C stretching vibrations. The bands at 1277 cm^{-1} is assigned to the Ar–O stretching vibrations, while the strong band at 1092 cm^{-1} give evidence for the presence of ionic perchlorate in each of the compound [30]. The bands at the region of 1005–621 cm^{-1} are assigned to the aromatic and aliphatic C–H bending vibrations. In addition, the band at about 479 and 463 cm^{-1} in the compound are assigned M–O and M–N stretching vibrations of 5-Brsalen, respectively [35].

3.3. UV–Vis spectrum and electrochemical property

UV–vis absorption spectrum is carried out for the complex **1** in CH_3CN solution to investigate the light absorption characteristics and the result is shown in Fig. 5. As can be seen, the complex **1** shows five absorption bands at 300–800 nm. The bands at ca. 409 and 354 nm may be due to ligand-to-metal charge transfer arising from 5-Brsalen ligand. The bands at around 316, 283 and 238 nm which appeared without considerable shifting compared to their parent ligands were assigned to the $\pi \rightarrow \pi^*$ transitions of the 5-Brsalen and 4,4-bipy ligands associated with the azomethine and aromatic ring systems, respectively [36,37]. Analytical data were also in good agreement with the proposed structures.

Cyclic voltammetry (CV) was carried out on **1** in MeCN solution at 293 K. The electrochemical behavior of **1** was examined in acetonitrile containing 0.1 M tetra-n-butylammonium hexafluorophosphate (Bu_4NPF_6) as a supporting electrolyte in a conventional three electrode configuration using a glassy carbon working electrode, Pt auxiliary electrode and Ag/AgCl reference electrode. A representative cyclic voltammogram of **1** is shown in Fig. 6, consisting of a reversible $\text{Mn}^{\text{III}}/\text{Mn}^{\text{II}}$ reduction at -0.34 V, and a quasi-reversible $\text{Mn}^{\text{III}}/\text{Mn}^{\text{IV}}$ metal-centered oxidation at $+1.34$ V versus aqueous Ag/AgCl. Moreover, the potential value for **1** ($E_{1/2}(1) = -0.18$ V, $E_{1/2}(2) = 0.60$ V), suggests relative stabilization of the Mn^{II} state and destabilization of the Mn^{IV} state, which is comparable to the closely related manganese(III) complexes [36,37].

3.4. Magnetic properties

The magnetic susceptibility of compound **1** was measured in the temperature range 2–300 K at a field strength of 1000 Oe. The temperature dependent magnetic behavior of **1** is shown in Fig. 7 as

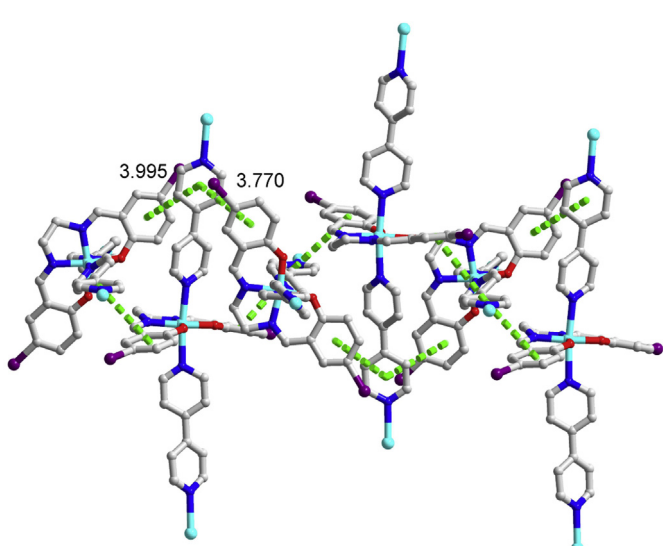


Fig. 2. Formation of two-dimensional supramolecular network by π -stacking interactions in compound **1**. All the H atoms, perchlorate anions and methanol molecules are omitted for clarity. Atomic scheme: Mn(III), turquoise; C, light gray; N, blue; Br, violet; O, red. (For interpretation of the references to color in this figure legend, the reader is referred to the web version of this article.)

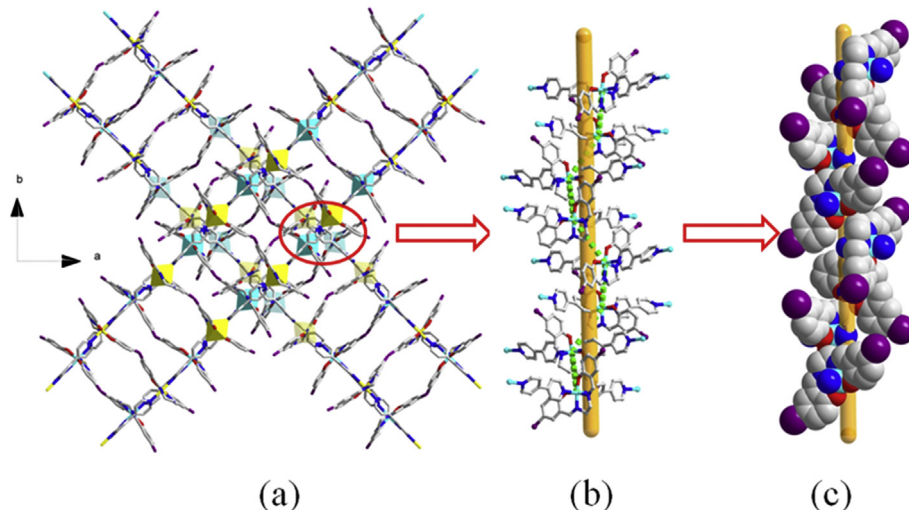


Fig. 3. (a) Perspective views of the multilayer chains of polyhedral scheme for **1** along the *a*-axis: First layer, yellow; Second layer, light yellow; third layer, turquoise; fourth layer, light turquoise. The hydrogen atoms, perchlorate anions and methanol molecules have been omitted for clarity. (b) Ball and stick representation of compound **1** viewed the helices along the *c* axis. The hydrogen atoms, perchlorate anions and methanol molecules have been omitted for clarity. (c) Perspective and space-filling viewed the helices in **1** along the *c* axis. The hydrogen atoms, anions, solvent and 4,4-bipy molecules are omitted for clarity. Atomic scheme: Mn(III), turquoise; C, light gray; N, blue; Br, violet; O, red. (For interpretation of the references to color in this figure legend, the reader is referred to the web version of this article.)

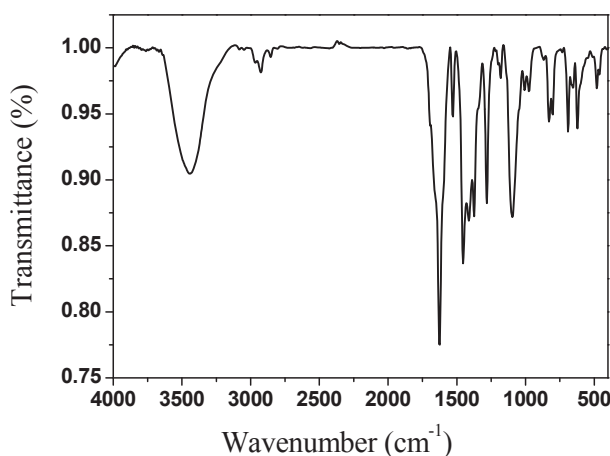


Fig. 4. IR spectra of compound **1**.

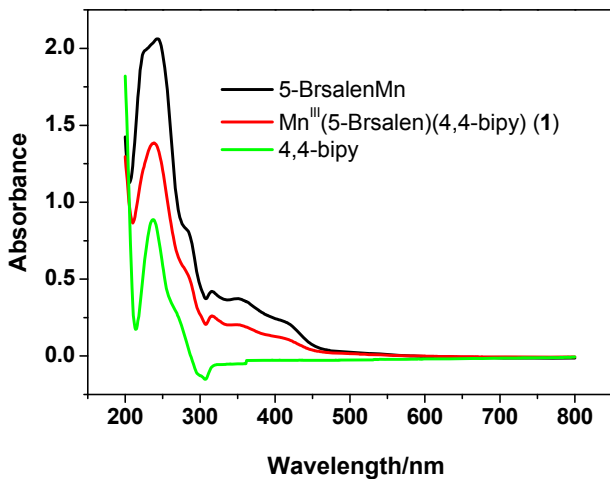


Fig. 5. UV-vis absorption spectrum of compound **1**, 5-BrsalenMn and 4,4-bipy ligands in CH_3CN solution(10^{-3} M).

χT versus T plots. The χT value ($2.93 \text{ cm}^3 \text{ mol}^{-1} \text{ K}$) at 300 K for the compound is lower than the calculated value ($3.0 \text{ cm}^3 \text{ mol}^{-1} \text{ K}$) for the uncoupled spins ($S = 2$) with $g = 2$. With a decrease of temperature from 300 K , the value of χT decreases very slowly to $2.85 \text{ cm}^3 \text{ mol}^{-1} \text{ K}$ at 10 K . On further lowering of the temperature, χT decreases sharply to $1.41 \text{ cm}^3 \text{ mol}^{-1} \text{ K}$ at 2.0 K . In most possible, the drop of magnetic susceptibility in χT form results from spin-orbit (SO) coupling of Mn(III) ion, since the neighboring Mn(III) ions are separated long distance. This temperature dependent magnetic behavior indicates weak antiferromagnetic interaction for the compound **1**.

4. Conclusion

We have synthesized a novel homochiral manganese (III) Mn(5-Brsalen) coordination polymer with left-handed helical character by spontaneous resolution on crystallization by using Mn(5-Brsalen) and 4,4-bipyridine. In compound **1**, each manganese(III)

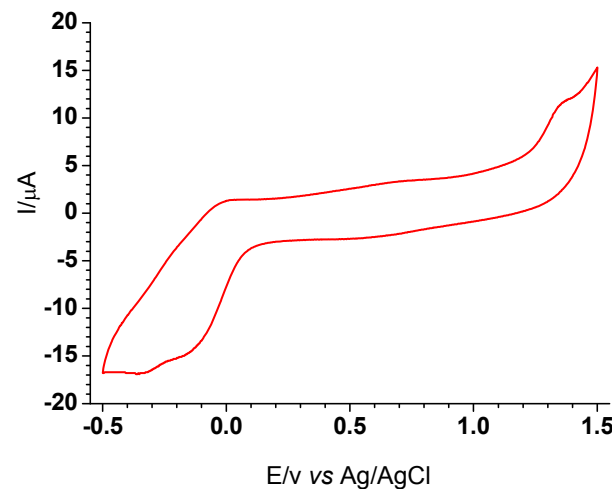


Fig. 6. Cyclic voltammogram of compound **1** in CH_3CN solution. Scan rate at 100 mV s^{-1} .

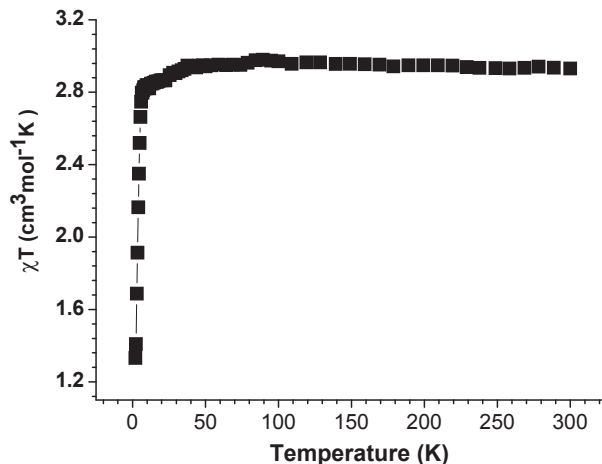


Fig. 7. Thermal variation of magnetic susceptibility, χT vs T (■) of compound 1 under an applied field of 1 kOe in the temperature range of 2–300 K.

anion is six-coordinate octahedral being bonded to four atoms of 5-Brsalen ligand in an equatorial plane and two nitrogen atoms from a 4,4-bipyridine ligand in axial positions. The structure of complex **1** can be described a supramolecular 2D-like structure which was formed by the intermolecular π -stacking interactions between the neighboring chains of the aromatic rings of 4,4-bipyridine and 5-Brsalen molecules. UV-vis absorption spectrum, electrochemistry and magnetic properties of the compound **1** have also been studied. Research on the other chiral Salen coordination polymer with the electrochemical property is currently underway.

Acknowledgment

This work was partly supported by the NSFC (Grant Nos. 21301023, 21501021, 11474045), the 2014 Program for Liaoning Excellent Talents in University (Grant No. LJQ2014138), and the Fundamental Research Funds for the Central Universities (Grant No. DC201502080305).

References

- [1] J. An, O.K. Farha, J.T. Hupp, E. Pohl, J.I. Yeh, N.L. Rosi, *Nat. Commun.* 3 (2012) 604–609.
- [2] M. Boiocchi, L. Fabbrizzi, *Chem. Soc. Rev.* 43 (2014) 1835–1847.
- [3] P. Wu, C. He, J. Wang, X. Peng, X. Li, Y. An, C. Duan, *J. Am. Chem. Soc.* 134 (2012) 14991–14999.
- [4] J.R. Li, J. Sculley, H.C. Zhou, *Chem. Rev.* 112 (2012) 869–932.
- [5] L.N. Li, J.X. Ma, C. Song, T.L. Chen, Z.H. Sun, S.Y. Wang, J.H. Luo, M.C. Hong, *Inorg. Chem.* 51 (2012) 2438–2442.
- [6] C.M. Liu, R.G. Xiong, D.Q. Zhang, D.B. Zhu, *J. Am. Chem. Soc.* 132 (2010) 4044–4045.
- [7] X. Jing, C. He, D. Dong, L. Yang, C. Duan, *Angew. Chem. Int. Ed.* 51 (2012) 10127–10131.
- [8] Y. Sameshima, N. Yoshinari, K. Tsuge, A. Igashira-Kamiyama, T. Konno, *Angew. Chem. Int. Ed.* 48 (2009) 8469–8472.
- [9] Z.M. Zhang, Y.G. Li, S. Yao, E.B. Wang, Y.H. Wang, R. Clérac, *Angew. Chem. Int. Ed.* 48 (2009) 1581–1584.
- [10] L. Pérez-García, D.B. Amabilino, *Chem. Soc. Rev.* 31 (2002) 342–356.
- [11] E.Q. Gao, Y.F. Yue, S.Q. Bai, Z. He, C.H. Yan, *J. Am. Chem. Soc.* 126 (2004) 1419–1429.
- [12] A. Bhattacharyya, B.N. Ghosh, S. Herrero, K. Rissanen, R. Jiménez-Aparicio, S. Chattopadhyay, *Dalton Trans.* 44 (2015) 493–497.
- [13] A. Bhattacharyya, S. Chattopadhyay, *RSC Adv.* 5 (2015) 18252–18257.
- [14] D.P. Dong, Z.G. Sun, F. Tong, Y.Y. Zhu, K. Chen, C.Q. Jiao, C.L. Wang, C. Li, W.N. Wang, *CrystEngComm* 13 (2011) 3317–3320.
- [15] D.P. Dong, L. Liu, Z.G. Sun, C.Q. Jiao, Z.M. Liu, C. Li, Y.Y. Zhu, K. Chen, C.L. Wang, *Cryst. Growth Des.* 11 (2011) 5346–5354.
- [16] Q. Li, X. Jiang, S. Du, *RSC Adv.* 5 (2015) 1785–1789.
- [17] P. Cui, L.J. Ren, Z. Chen, H.C. Hu, B. Zhao, W. Shi, P. Cheng, *Inorg. Chem.* 51 (2012) 2303–2310.
- [18] Y.L. Gai, F.L. Jiang, K.C. Xiong, L. Chen, D.Q. Yuan, L.J. Zhang, K. Zhou, M.C. Hong, *Cryst. Growth Des.* 12 (2012) 2079–2088.
- [19] L.S. Long, *CrystEngComm* 12 (2010) 1354–1365.
- [20] S.I. Vagin, R. Reichardt, S. Klaus, B. Rieger, S. Chattopadhyay, *J. Am. Chem. Soc.* 132 (2010) 14367–14369.
- [21] R. Herchel, Z. Šindelář, Z. Trávníček, R. Zbořil, J. Vančo, *Dalton Trans.* (2009) 9870–9880.
- [22] J. Cisterna, V. Dorcet, C. Manzur, I. Ledoux-Rak, J.R. Hamon, D. Carrillo, *Inorg. Chim. Acta* 430 (2015) 82–90.
- [23] H. Zhou, Y. Wang, F. Mou, X. Shen, Y. Liu, *Polyhedron* 85 (2015) 457–466.
- [24] G. Li, X. Xi, W. Xuan, T. Dong, Y. Cui, *CrystEngComm* 12 (2010) 2424–2428.
- [25] T. Miao, Z. Zhang, W. Feng, P. Su, H. Feng, X. Lü, D. Fan, W. Wong, R.A. Jones, C. Su, *Spectrochim. Acta Part A Mol. Biomol. Spectrosc.* 132 (2014) 205–214.
- [26] X. Yang, R.A. Jones, S. Huang, *Coord. Chem. Rev.* 273–274 (2014) 63–75.
- [27] M. Ferbinteanu, H. Miyasaka, W. Wernsdorfer, K. Nakata, K. Sugiyama, M. Yamashita, C. Coulon, R. Clérac, *J. Am. Chem. Soc.* 127 (2005) 3090–3099.
- [28] R. Clérac, H. Miyasaka, M. Yamashita, C. Coulon, *J. Am. Chem. Soc.* 124 (2002) 12837–12844.
- [29] H. Miyasaka, A. Saitoh, S. Abe, *Coord. Chem. Rev.* 251 (2007) 2622–2664.
- [30] A. Bhattacharyya, S. Sen, K. Harms, S. Chattopadhyay, *Polyhedron* 88 (2015) 156–163.
- [31] H.J. Choi, J.J. Sokol, J.R. Long, *Inorg. Chem.* 43 (2004) 1606–1608.
- [32] G.M. Sheldrick, *Acta Crystallogr. Sect. A* 64 (2008) 112.
- [33] X.D. Chen, M. Du, T.C.W. Mak, *Chem. Commun.* (2005) 4417–4419.
- [34] R.Q. Zou, R.Q. Zhong, M. Du, D.S. Pandey, Q. Xu, *Cryst. Growth Des.* 8 (2008) 452–459.
- [35] A. Ghaffari, M. Behzad, M. Pooyan, H.A. Rudbari, G. Bruno, *J. Mol. Struct.* 1063 (2014) 1–7.
- [36] Z. Abbas, M. Behzad, A. Ghaffari, H.A. Rudbari, G. Bruno, *Inorg. Chim. Acta* 414 (2014) 78–84.
- [37] S. Biswas, A.K. Dutta, K. Mitra, M.C. Dul, S. Dutta, C. Lucas, B. Adhikary, *Inorg. Chim. Acta* 377 (2011) 56–61.